Nanoscale

Accepted Manuscript

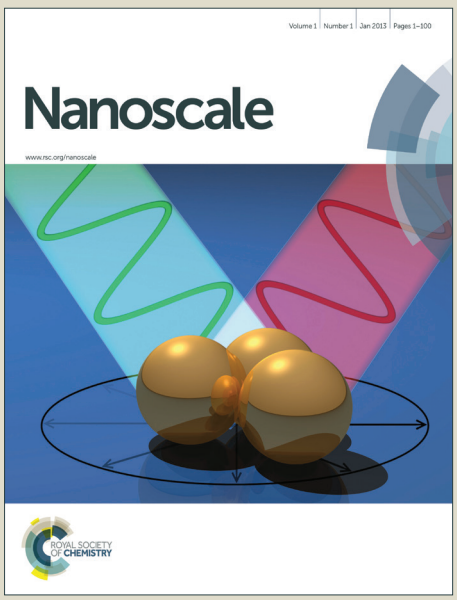

ROYAL SOCIETY OF CHEMISTRY

www.rsc.org/nanoscale

Cite this: DOI: 10.1039/c0xx00000x

www.rsc.org/xxxxxx

ARTICLE TYPE

Bandgap engineering and manipulating electronic and optical properties of ZnO nanowires by uniaxial strain

Rui-wen Shao,[a] Kun Zheng,[a]* Bin Wei,[a] Yue-fei Zhang,[a] Yu-jie Li,[a] Xiao-dong Han,[a] Ze Zhang,[b] and Jin Zou [c]*

Received (in XXX, XXX) Xth XXXXXXXXX 200X, Accepted Xth XXXXXXXXX 200X

DOI: 10.1039/b000000x

Abstract

Bandgap engineering is a common practice for tuning semiconductors for desired physical properties. Although possible strain effects in semiconductors have been investigated for over a half-century, a profound understanding of their influence on energy bands, especially for large elastic strain remains unclear. In this study, a systematic investigation of transport property of n-type [0001] ZnO nanowires was performed at room temperature using *in-situ* scanning tunnelling microscope-transmission electron microscope technique that show the transport property varies with applied external uniaxial strain. It has been found that the resistance of ZnO nanowire decreases continuously with increasing the compressive strain, but increases under the increased tensile strain, suggesting the piezo-resistive characteristic. A series of near-band-edge emissions were measured and the corresponding varieties of bandgaps were obtained during the tensile process of individual ZnO nanowires via cathodoluminescence spectroscopy. From which, a relationship between the changes of energy bandgap and the transport property, both induced by uniaxial strain, is built.

The bandgap energy (E_g) of a semiconductor determines its physiochemical properties, and because of this, a great deal of interest has been devoted to the bandgap engineering as a powerful technique for developing new semiconductor materials, particularly at the nanoscale. Bandgap engineering refers to a process of controlling E_g of a semiconductor, usually adjusted by its chemical composition. However, recent strain-induced bandgap engineering of semiconducting nanostructures has attracted much attention,[1-4] since nanostructured materials provide a novel approach for bandgap modulation through their tuneable sizes and shapes due to the quantum confinement effects.[5-7] Moreover, the high elastic limit of semiconducting nanostructures induces a larger tuneable E_g range in comparison to what is possible with their bulk counterparts.[8,9]

Although ZnO nanostructures have been used in many applications where strain engineering plays a role, such as nanogenerators,[10,11] nanowire (NW) field effect transistors,[12] piezo-electric diodes[13] and chemical sensors.[14] However, it is still not clear that how the band structure variation induced by strain relates to electrical response due to the difficult to separate the contribution of piezo-resistive and piezo-electric effects.[15,16] To understand the strain effect on the band structure and corresponding transport properties of ZnO NWs, the influence of the piezo-electric effect should be eliminated. Several studies have been carried out for this purpose. Yang *et al.*[17,18] synthesized Sb-doped ZnO NWs, and obtained the resistance variation with increasing the applied strain. By making Ohmic contacts between NWs and electrodes, Han *et al.*[19] observed a large increase in electrical conductance of ZnO NWs induced by bending strain. In addition, strain-luminescence measurement techniques for NWs have been developed, such as cathodoluminescence (CL),[20-22] photoluminescence,[9,23,24] and Raman spectroscopy,[25] in order to reveal the strain effect on their band structures. However, most previous studies were based on bent NWs that contain a mixture of tensile and compressive strain states, making it difficult to establish the quantitative relationship between the physical property change and the applied strain. Despite that theoretical calculations on the bandgap shifts of strained NWs, including uniaxial compressive and tensile states, have been widely investigated,[26,27] there were a limited reports on the alternation of bandgap changes and transport properties under both uniaxial tensile and compressive strains for [0001] ZnO NWs.

In this study, the relationship between bandgap variation and the change of transport properties, both induced by the strain, was established via two correlated experiments. In the first experiment, the transport properties of typical ZnO NWs were measured through the *in-situ* deformation process in a transmission electron microscope that provide a relationship between strain and electric conductance. In the second experiment, the change of near-band-edge (NBE) emission of typical ZnO NWs caused by strain were measured in a scanning electron microscope (SEM) that give the variation of E_g with different uniaxial tensile strains. By correlating these two experiments, the variations of transport properties as a function of E_g, under tensile strain, is established, from which, high sensitivity of transport properties as a function of E_g can be obtained.

[0001] ZnO NWs used in this study were grown by the chemical-vapor-deposition (CVD) method,[28,29] without intentionally doping. Nevertheless, due to the common presence of H impurities,[30] O vacancies,[31] and Zn interstitials[32] in CVD grown NWs, we anticipate that our ZnO NWs exhibit a n-type characteristic.

The *in-situ* electrical measurement were performed using a commercial scanning tunnelling microscope-transmission electron microscope probing system (STM-TEM, Nanofactory Instruments)[33] inserted into a JEOL-2010 TEM (operated at 200kV). Before the *in-situ* experiment, two fresh and sharp W tips were respectively fixed on the movable end of a piezo-motor and on a fixed Ag electrode. The former can be moved precisely in three dimensions. Figure 1(a) is a schematic drawing of the experimental setup, in which a NW is bonded to the two W electrode tips by the electron beam induced deposition (EBID). Detailed process can also be found in Refs. 34 and 35. By accurately controlling the piezo-motor, the individual NWs can be either stretched or compressed. Figure 1(b) is a low magnified TEM image showing two W electrode tips and a bonded ZnO NW.

In this study, W tips were chosen to fabricate electrodes since its work function (4.55eV) is very close to the electron affinity of ZnO (4.2~4.5eV).[36-38] In order to achieve good electrical contacts between the ZnO NWs and the W electrodes, the W tips were freshly prepared and a large current was firstly introduced to eliminate the oxide layers on the surfaces of W tips. After this fast melt-quench process, the sharp points of the W tips became hemispherical shape, as shown in the inset of Figure 1(b). EBID was used then to weld the NW and two W electrodes.

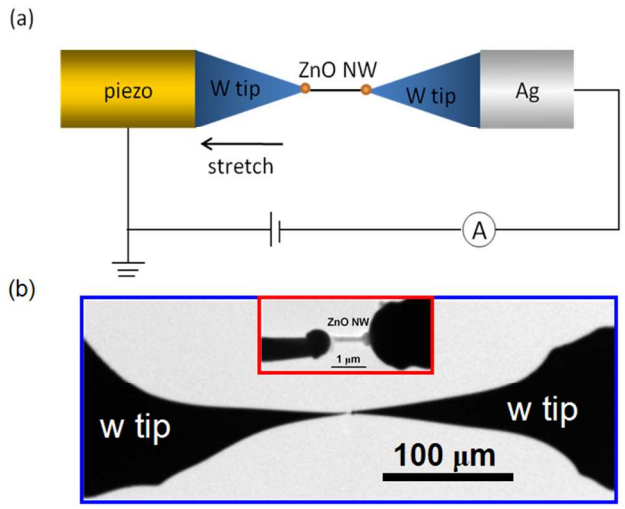

Figure 1. (a) Experimental setup showing a NW connected with W electrode tips placed inside a STM-TEM probing system; (b) W electrode tips (movable electrode and fixed electrode) and a bonded ZnO NW.

Figure 2(a) shows a typical strain-free ZnO NW with a length of 822 nm and a width of 136 nm, respectively. By controlling the piezo-motor movement (by careful calibration, each fine step corresponding a movement of 0.6 nm), the ZnO NW can be either stretched or compressed, and the corresponding *I-V* measurements can be carried out simultaneously by applying an external voltage under a given strain to explore the intrinsic piezo-resistance of strained n-type [0001] ZnO NWs.

Since the piezo-motor can be accurately controlled forwards and backwards and its repeatability was carefully examined and confirmed, we designed the *in-situ* experiment as follows. After taken the TEM image of Figure 2(a), the electron beam was turned off, the deformations (compressed or stretched) were achieved by changing 8 fine steps of the piezo-motor for each deformation. For each deformation, its corresponding *I-V* characteristic was measured by sweeping the voltage from -2 to 2 V. This procedure eliminates the electron beam effect on the measured *I-V* characteristics. After that, the entire experiment was repeated (with identical deformation-controlled by repeating the steps of the piezo-motor) with the electron beam being switched on (weak, but sufficient for taking TEM images), in which the *I-V* characteristics were measured again and the corresponding TEM images of strained ZnO NW were recorded simultaneously. It has been found that the *I-V* characteristics were identical for each deformation, suggesting that the electron-beam effect is minimal in our experiments. Besides, to eliminate the influence of the piezo-electric effect[15] completely, the *I-V* measurements were performed by waiting for several min after each deformation, since the piezo-electric contribution is time-dependent and the polar charges produced by the piezo-electric effect can be neutralized by external free charges from the grounded electrode.[10,11]

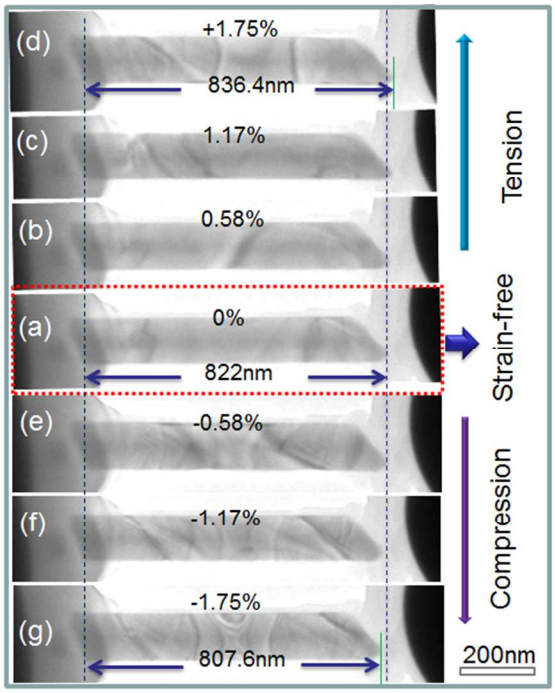

Figure 2. TEM images showing the ZnO NW with (a) unstrained state; (b-d) tensile deformed; (e-g) compressively deformed.

Figures 2(b)~(d) show 3 sequential TEM images of the ZnO NW under the tensile strain, each with 4.8 nm elongation when compared with the previous one. Therefore, the lengths of the ZnO NW are respectively 826.8 nm for (b), 831.6 nm for (c), and 836.4 nm for (d), which correspond to tensile strains of 0.58% for (b), 1.18% for (c), and 1.75% for (d), respectively. On the other hand, Figures 2(e)~(g) show 3 sequential TEM images of the ZnO NW under different compressive strains with an interval step of 4.8 nm, which correspond to compressive strains of -

0.58% for (e), -1.18% for (f), and -1.75% for (g), respectively. In order to avoid to potential buckling or plastic deformation, a small uniaxial strain (< 2%) is applied. In our case, the strain is uniform due to the small aspect ratio of length-diameter (about 5) of the ZnO NW. Under these conditions, the strain distribution was simulated by using finite element method (See Supplementary Information).

For each deformation state (including the strain-free case – Figure 2(a)), *I-V* characteristic was measured by sweeping the voltage from -2 to 2 V. Figure 3 summaries these *I-V* characteristics. Since black solid line shows the initial transport property of the strain-free ZnO NW, which can be used as a benchmark to evaluate the change of conductance of the ZnO NW under strain. As can be seen from Figure 3, with increasing the tensile strain, the conductance is enhanced, as illustrated by dashed curves (indicated by blue arrow); while, on the other hand, with increasing the compressive strain, conductance is decreased as shown by the solid curves (indicated by red arrow).

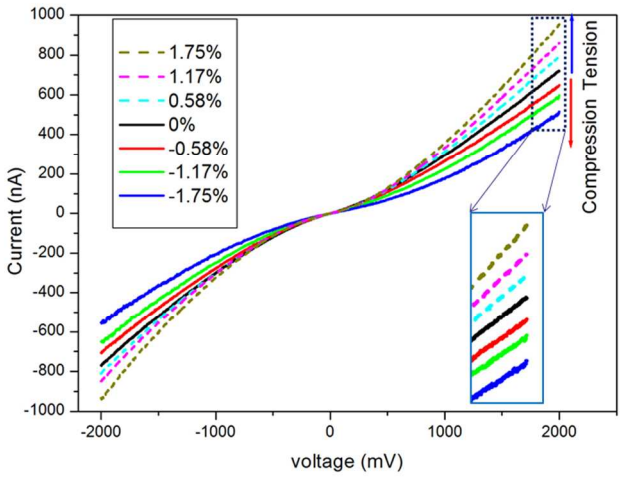

Figure 3. Corresponding *I-V* characteristics of Figure 2; the insert is enlarge region of the dashed frame region.

To clarify the fundamental reason that is responsible for the strain-induced conductance variation, we need to consider both piezo-resistive and piezo-electric effects of ZnO respectively due to its polar and semiconducting dual characteristics.[10-12] For polar crystals, such as ZnO, the potential piezo-electric effect caused by strain cannot be simply ignored. When such a polar crystal is mechanically deformed, the positive- and negative-charged centers are displaced with respect to each other, so that, although the overall crystal remains electrically neutral, the difference in charge-center displacements result in an electric polarization within the crystal.[10] Hu *et al.*[16] found that the conductance of ZnO NWs, dominated by the piezo-electric effect, decreased with increasing the strain regardless of whether the ZnO NWs were under compressive or tensile strains. This is quite different from our results, suggesting that the transport properties found in our ZnO NWs should not be caused by the piezo-electric effect. On the other hand, the strain induced variation of a bandgap, i.e. the piezo-resistive effect, does exists in all semiconductors, so that the piezo-resistive effect should dominate the variation of transport properties found in our ZnO NWs.

To understand the piezo-resistive effect caused *I-V* characteristics as a function of the applied strains (compressive and tensile), the relationship between the resistivity and the applied strain is established (the detailed establishment can be found in Supplementary Information) and shown in Figure 4, from which (1) a linear relationship can be seen and (2) the resistivity decreases with increasing the tensile strain and increases with increasing the compressive strain. Since the gauge factor (*GF*) of piezo-resistance can be expressed as[2]

$$\frac{\Delta R}{R} = GF\frac{\Delta l}{l}, \quad (1)$$

where R is the resistance and l is the original length, *GF* of the NW can be determined to be -14, which can be used to calculate the piezo-resistance coefficient (π) (and vice versa) from:

$$GF = \pi Y, \quad (2)$$

where Y is the Young's modulus of the [0001] ZnO NW. Using Y = 160 GPa,[39] π= -8.75×10^{-11} Pa^{-1} can be obtained for the ZnO NW, which shows no significant difference compared with the reported piezo-resistance coefficient of single ZnO NW.[19] It is of interest to note that the obtained π (-8.75×10^{-11} Pa^{-1}) is about 8 times higher than that of the SiC NWs,[34] suggesting that ZnO NWs should be more strain sensitivity than SiC NWs.

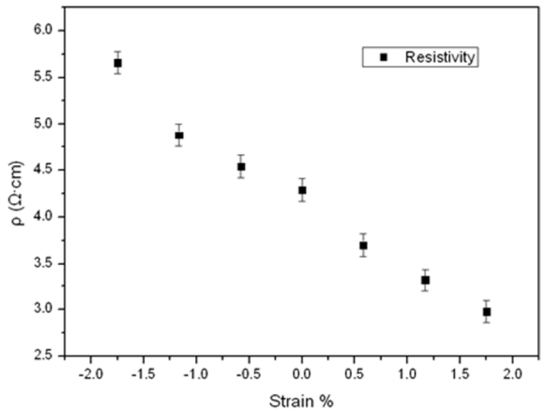

Figure 4. The relationship of the resistivity as a function of the applied strain.

To determine the observed transport properties variation of our ZnO NWs as a function of strain, we note that, for a semiconductor, strain can change the band structure,[2] carrier concentrations and motilities,[12] which may significantly affect the transport properties. Mathematically, the resistivity (ρ) of a ZnO NW can be expressed as[40]

$$\rho = \frac{1}{ne\mu}, \quad (3)$$

where n is the carrier concentration, e is the electrical charge, and μ is the electron mobility. Based on a well-established model,[41-44] n and μ can be retrieved from the experimental *I-V* curve (details see Supplementary Information). The results are shown in Figure 5. Our calculation indicates that the electron mobility μ increases with increasing the tensile strain and decreases with increasing the compressive strain, however, the electron concentration n varied slightly with both tensile and compressive strains. This indicates that the change of resistivity is mainly resulted from the

variation of electron mobility which is similar to the Si NWs.[2,45,46] Han *et al.*[19] observed a large increase in electrical conductance of ZnO NWs induced by bending strain, and proposed that the tensile strain could narrow the bandgap, increase the concentration of electrons with low effective mass in the axial direction which finally enhance the electron mobility and in turn result in the observed conductance enhancement. Their result also suggests that E_g increases with increasing the compressive strain, but decreases with increasing the tensile strain. In fact, this strain-E_g relationship has been predicted by theoretical modelling.[26,27] Nevertheless, the detailed relationship between conductance and E_g under the uniaxial strain should be clarified.

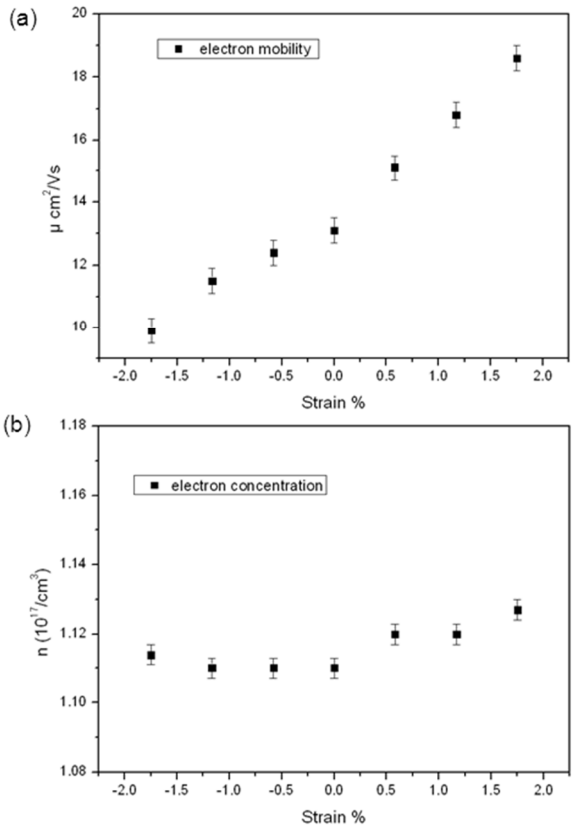

Figure 5. (a) The variation of the electron concentration n, and (b) the variation of the carrier mobility μ, both as a function of the applied strain.

To confirm the impact of the uniaxial strain on the energy band of ZnO NWs, we measured the change of the CL's NBE emission of ZnO NWs in a SEM (operated at 15kV) under uniaxial tensile strain, in which, for a given ZnO NW, CL spectra under different tensile strains were collected at room temperature with a beam current of 10^{-8} to 10^{-9}A and a spectral shift of less than 0.5 nm with a UV-NIR blazed grating of 0.1 to 0.4 nm. The detailed experimental setup can be found in Ref. 47. Figure 6(a) shows the variations in the NBE peak of a stretched NW with a tensile strain up to 2.6%. Clearly, the NBE peak moves towards the lower energies as a result of tensile strain, corresponding to a variation of E_g from 3.270 eV (strain-free) to 3.248 eV (2.6% tensile strain), resulted in an overall E_g variation of 22 meV. Figure 6(b) shows the variation of E_g as a function of the tensile strain.

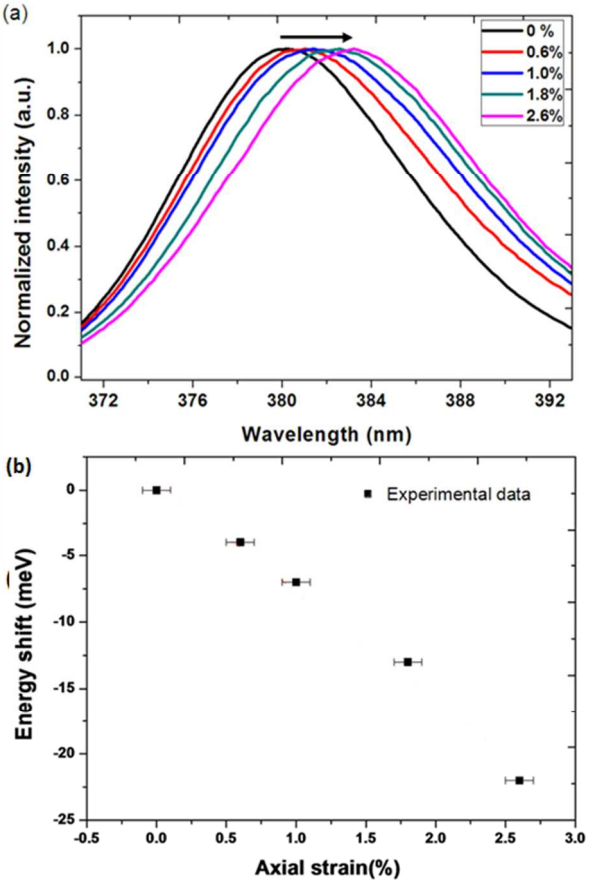

Figure 6. (a) Normalized CL spectra of one single suspended ZnO NW subject to increasing strain. For increasing tensile strain, the spectrum shifts toward higher wavelength, up to 383 nm^{-1}, corresponding to 2.6% tensile strain. (b) The energy shifts and strain values for each of the spectra.

From Figures 4 and 6(b), the variations of the conductance as a function of E_g under uniaxial tensile strain can be determined, as plotted in Figure 7. As can be seen, with decreasing E_g (induced by tensile strain), the conductance increases monotonically. From Figure 7, a small E_g variation (such as 22 meV, compared with its original E_g of 3.27eV) can lead to an over 40% increase in its conductance, suggesting that our ZnO NWs are indeed very sensitive to strain induced variation of E_g and thus conductivities. This unique feature suggests that our ZnO NWs should be an ideal candidate in strain-sensitive applications.

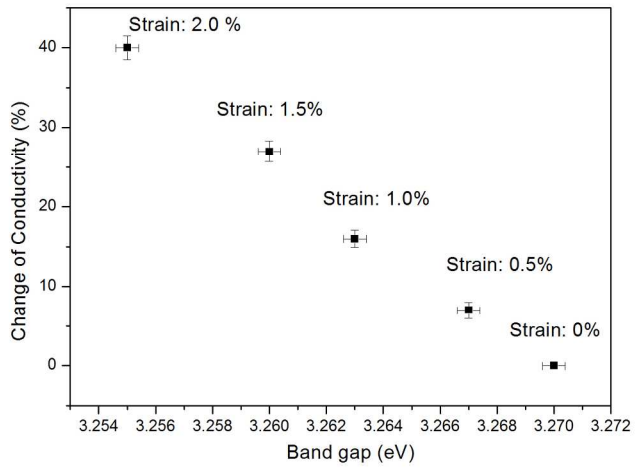

Figure 7. The variations of the conductance as a function of E_g under uniaxial tensile strain

In summary, we performed *in-situ* manipulation and electrical and optical measurements on individual n-type [0001] ZnO NWs. Variations of the conductance and the NBE emission of ZnO NWs are witnessed under uniaxial strain. It has been found that (1) the conductance change of the ZnO NWs decreases with increasing the applied strain (compressive strain refers to negative strain) up to 2%, and (2) E_g also decreases with increasing the applied tensile strain. The correlation between the variations of conductance and E_g as a function of tensile strain leads to the clarification of the relationship between conductance as a function of E_g, from which the conductance is found to be very sensitive to strain induced E_g. This study provides a new approach to tune the electrical and optical properties in ZnO NWs.

Acknowledgments

This work was supported by the National Natural Science Foundation of China (11004004, 11374029), the Beijing Municipal Natural Science Foundation (1112004), A Foundation for the Author of National Excellent Doctoral Dissertation of PR China, Beijing Nova Program (Z121103002512017), the Key Project of National Natural Science Foundation of China (11234011) and (50831001), and Australian Research Council.

Notes and references

[a] *Institute of Microstructure and Properties of Advanced Materials, Beijing University of Technology, Beijing 100124, China. E-mail: kunzheng@bjut.edu.cn;*

[b] *Department of Materials Science, Zhejiang University, Hangzhou, Zhejiang 310058, China;*

.[c] *Material Engineering and Centre for Microscopy and Microanalysis, The University of Queensland, Brisbane, QLD 4072, Australia. E-mail: j.zou@uq.edu.au*

† Electronic Supplementary Information (ESI) available: [details of any supplementary information available should be included here]. See DOI: 10.1039/b000000x/

1 M. Ieong, B. Doris, J. Kedzierski, K. Rim and M. Yang, *Science*, 2004, **306**, 2057.
2 R. He and P. Yang, *Nat. Nanotechnol.,* 2006, **1**, 42.
3 M. M. Roberts, L. J. Klein, D. E. Savage, K. A. Slinker, M. Friesen, G. Celler, M. A. Eriksson and M. G.Lagally, *Nat. Mater.*, 2006, **5**, 388.
4 T. W. Tombler, C. Zhou, L. Alexseyev, J. Kong, H. Dai, L. Liu, C. S. Jayanthi, M. Tang and S. Y. Wu, *Nature*, 2000, **405**, 769.
5 D. D. D. Ma, C. S. Lee, F. C. K. Au, S. Y. Tong and S. T. Lee, *Science*, 2003, **299**, 1874.
6 J. Sun, W. E. Buhro, L.-W. Wang and J. Schrier, *Nano Lett.* 2008, **8**, 2913.
7 X. Wang, Y. Z. Jin, H. P. He, F. Yang and Z. Z. Ye, *Nanosclae*, 2013, **21**, 6464.
8 Y. Li, F. Qian, J. Xiang and C. M. Lieber, *Mater Today,* 2006, **9**, 18.
9 G. Signorello, S. Karg, M. T. Björk, B. Gotsmann and H. Riel. Nano Lett., 2013, **13**, 917.
10 Z. L. Wang and J. H. Song, *Science,* 2006, **312**, 242.
11 X. D. Wang, J. H. Song, J. Liu and Z. L. Wang, *Science,* 2007, **316**, 102.
12 X. D. Wang, J. Zhou, J. H. Song, J. Liu, N. S. Xu and Z. L. Wang, *Nano Lett*. 2006, **6**, 2768.
13 J. H. He, C. L. Hsin, J. Liu, L. J. Chen and Z. L. Wang, *Adv. Mater*., 2007, **19**, 781.
14 C. S. Lao, Q. Kuang, Z. L. Wang, C. M. Park and Y. Deng, *Appl. Phys. Lett.*, 2007, **90**, 262107.
15 J. Zhou, Y. D.Gu, P. Fei, W. J. Mai,Y. F.Gao, R. S. Yang, G. Bao and Z. L. Wang, *Nano Lett*., 2008, **8**, 3035.
16 Y. F. Hu, Y. L. Chang, P. Fei, R. L. Snyderand Z. L. Wang, *ACS Nano*., 2010, **4**, 1234.
17 Y. Yang, J. J. Qi, Y. Zhang, Q. L. Liao, L. D. Tang and Z. Qin, *Appl. Phys. Lett.*, 2008, **92**, 183117.
18 Y. Yang, J. J. Qi, W. Guo, Q. L. Liao, and Y. Zhang, *Cryst. Eng. Comm.*, 2010, **12**, 2005.
19 X. B. Han, G.Y. Jing, X. Z. Zhang, R. M. Ma, X. F. Song, J. Xu, Z. M. Liao, N. Wang and D. P. Yu, *Nano Res*,. 2009, **2**,553.
20 X. B. Han, L. Z. Kou, X. L. Lang, J. B. Xia, N. Wang, R. Qin, J. Lu, J. Xu, Z. M. Liao, X. Z. Zhang, X. D. Shan, X. F. Song, J. Y. Gao, W. L. Guo and D. P. Yu, *Adv. Mater.*, 2009, **21**, 4937.
21 X. B. Han, L. Z. Kou, Z. H. Zhang, Z. Y. Zhang, X. L. Zhu, J.Xu, Z. M. Liao, W. L. Guo and D. P. Yu, *Adv. Mater.*, 2012, **24**, 4707.
22 Q. Fu, Z. Y. Zhang, L. Z. Kou, P. C. Wu, X. B. Han, X. L. Zhu, J. Y. Gao, J. Xu, Q. Zhao, W. L. Guo and D. P. Yu, *Nano Res.*, 2011, **4**, 308.
23 M. Montazeri, M. Fickenscher, L. M. Smith, H. E. Jackson, J. Yarrison-Rice, J. H. Kang, Q. Gao, H. H. Tan, C. Jagadish, Y. N. Guo, J. Zou, M. E. Pistol and C. E. Pryor, *Nano Lett.,* 2010, **10**, 880.
24 H. Maki, T. Sato and K. Ishibashi, *Nano Lett.,* 2007, **7**, 890.
25 J. N. Chen, G. Conache, M. E. Pistol, S. M. Gray, M. T. Borgstrom, H. X. Xu, H. Q. Xu, L. Samuelson and U. Hakanson, *Nano Lett.,* 2010, **10**, 1280.
26 S. Li, Q. Jiang, G. W. Yang, *Appl. Phys. Lett.*, 2010, **96**, 213101.
27 Y. R. Yang, X. H. Yan, X. Yang, and D. Lu, *Appl. Phys. Lett.*, 2010, **97**, 033106.
28 X. C. Bian, C. Q. Huo, Y. F. Zhang and Q. Chen, *Front. Mater. Sci. China* 2008, **2**, 31.
29 L. H. Wang, X. D. Han, Y. F. Zhang, K. Zheng, P. Liu and Z. Zhang, *Acta Mater.,* 2011,**59**, 651.

30 C. G. Van de Walle, *Phys. Rev. Lett,*, 2000, **85**, 1012.
31 E. C. Lee, Y. S. Kim, Y. G. Jin and K. J. Chang, *Phys. Rev. B,* 2001, **64**, 085120.
32 A. F. Kohan, G. Ceder, D. Morgan and C. G. Van de Walle , *Phys. Rev. B*, 2000, **61**, 15019.
33 K. Svensson, Y. Jompol, H. Olin and E. Olsson, *Rev.Sci. Instrum*., 2003,**74**, 4945.
34 R. W. Shao, K. Zheng, Y. F. Zhang, Y. J. Li, Ze. Zhang and X. D. Han, *Appl. Phys. Lett.*, 2012, **101**, 233109.
35 K. Zheng, R. W. Shao, Q. S. Deng, Y. F. Zhang, Y. J. Li, X. D. Han, Z. Zhang, and J. Zou, *Appl. Phys. Lett.* Accepted, 2014
36 S. Hasegawa, S. Nishida, T. Yamashita and H. Asahi, *J. Ceramic Proc. Res.,* 2005, **6**, 245.
37 J. H. He, S. T.Ho, T. B. Wu, L. J. Chen and Z. L. Wang, *Chemical Physics Letters,*2007, **435,** 119.
38 H. Kobayashi, H. Mori, T. Ishida and Y. Nakato, *J. Appl. Phys.*, 1995, 77, 1301
39 C. Q. Chen, Y. Shi, Y. S. Zhang, J. Zhu and Y. J. Yan, *Phys. Rev. Lett.,* 2006, **96**, 075505.
40 S. M. Sze, Physics of Semiconductor Devices, 2nd ed. (Wiley, New York, 1981).
41 Z. Y. Zhang, C. H. Jin, X. L. Liang, Q. Chen and L.-M. Peng, Appl. Phys. Lett., 2006, 88, 073102.
42 K. H. Liu, P. Gao, Z. Xu, X. D. Bai and E. G. Wang. Appl. Phys. Lett., 2008, 92, 213105.
43 X. D. Bai, D. Golberg, Y. Bando, C.-Y. Zhi, C.-C. Tang, M. Mitome and K. Kurashima. Nano Lett., 2007, 7, 632.
44 Z.-Y. Zhang, K. Yao, Y. Liu, C.-H. Jin, X.-L. Liang, Q. Chen and L.-M. Peng. Adv. Funct. Mater., 2007, 17 , 2478.
45 Y. M. Niquet, C. Delerue and C. Krzeminski, Nano Lett., 2012, 12, 3545.
46 M. V. Fishchetti, and S. E. Laux, J. Appl.Phys., 1996, 80, 2234.
47 B. Wei, K. Zheng, Y. Ji, Y. F. Zhang, Z. Zhang and X. D. Han, *Nano Lett.* 2012,**12** 4595.